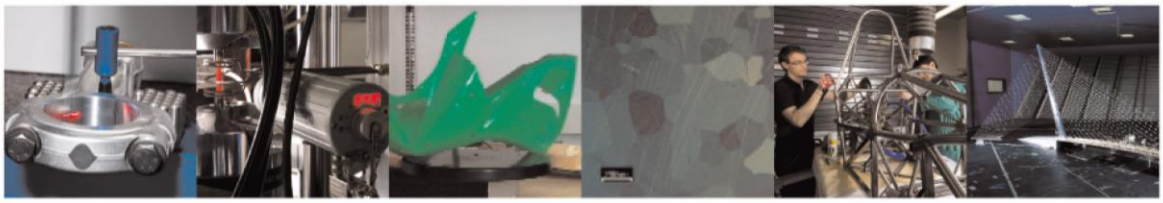

Effects of Mold Cavity Geometry on Flow Rate and Mechanical Properties in Al-Si-Mg Alloy

Tansel Tunçay, Furkan Baytar, Badegül Tunçay, Talha Sunar & Derya Dişpinar

This is a post-peer-review, pre-copyedit version of an article published in Journal of Materials Engineering and Performance. The final authenticated version is available online at: http://dx.doi.org/10.1007/s11665-022-07412-0

Effects of Mold Cavity Geometry on Flow Rate and Mechanical Properties in Al-Si-Mg Alloy

Tansel TUNÇAY[1], Furkan BAYTAR[1], Badegül TUNÇAY[1], Talha SUNAR[1] and Derya DIŞPINAR[2]

[1] Karabuk University, Technology Faculty,
Manufacturing Engineering Department, Balıklarkayası, Karabuk, Turkey
[2] Foseco, R&D Non-ferrous Metal Treatment, Enschede,
tanseltuncay@karabuk.edu.tr, furkanbaytar54@gmail.com, badegultuncay@gmail.com,
talhasunar@karabuk.edu.tr, derya.dispinar@vesuvius.com

ABSTRACT

In this study, the effects of the oxide films formed by using different mold cavity geometries on the mechanical properties of the parts were investigated. The casting process was carried out using the same runner system with different mold geometries. The effect of liquid metal flow rate on bifilm formation and the mechanical properties of the cast material was examined. Eventually, oxide bifilms formed in the mold cavity when the flow rate is low (caused by folding). These oxide bifilms negatively affect the mechanical properties as much as the oxide bifilms formed in the runner system. When real-time liquid metal flow rates are examined in different casting cavities, flow irregularities such as turbulence, folding, and splashing were developed differently in the flow rate of the liquid metal. It was determined that the stability in the flow rate of the liquid metal directly affects the mechanical strength.

Keywords: Casting runner system, flow rate, microstructure, mechanical properties.

1. Introduction

The casting method is the most traditional metal forming technology known. Although it competes with different production methods, it is still preferred today due to its familiarity and ease of application. The Casting production method; basically consists of two basic physical phenomena. The first is transferring the liquid metal to the mold cavity with the appropriate runner system, and the second is solidifying the liquid metal in the mold cavity (Ref 1,2). Preventing the oxidation of the liquid metal while the liquid metal fills the mold cavity reduces the number of inclusions and oxides in the solidified casting material (Ref 3). In many cases, only the dross formed on the surface is considered a critical defect; therefore, it is skimmed off before casting. On the other hand, another critical parameter is the folding of the liquid front during pouring and mold filling. These defects are known as bifilms. Mechanical properties of the cast material may vary depending on the amount of oxide bifilm (Ref 4,5). In the casting pouring basin (counterbore), vortex, i.e., air suction, is inevitable during the movement of the liquid metal into the mold cavity. There should be obstacles and stoppers in the casting pouring basin to minimize this (Ref 1–6). The location of the runner system of the cast part (top or bottom) affects the mechanical properties (Ref 7). Liquid metal accelerates in the vertical runner system depending on the drop height. Despite the speed it gains in the vertical runner, the liquid metal is pushed back by the air in the mold cavity. Nevertheless, the critical parameter is the natural geometry of the falling liquid, which narrows, so the liquid metal cross-sectional area in the sprue is tapered, and the vertical runner system narrows. As the liquid metal falling from the vertical runner fills the mold cavity, the flow rates change depending on the increasing liquid metal level in the mold cavity and time. In

addition, it is necessary to combine the cross-section change between the basin and the sprue with a radius. A diffuser changes the horizontal runner cross-section area to reduce the liquid metal velocity on the horizontal runner. Hsu et al. have carried out several designs to prevent oxide and bifilm entrainment into the cast part (Ref 8–10). The mechanical properties of the cast material vary depending on the speed of the liquid metal, the shape of the gating system elements, and the cross-sectional area. The critical gate (ingate) entry velocity for aluminum and its alloys is known as 0.5 m/s (Ref 9–11). Ceramic filters used in the runner system reduce the oxide bifilm content and decrease the liquid metal's velocity, thereby improving the cast material's mechanical properties while reducing the flow rate (Ref 12). Hsu and Li (Ref 13) investigated the effects of ceramic foam filters positioned on three different gating systems on bifilm formation and the velocity of liquid metal and noted that ceramic foam filters had a positive effect. Metzloff et al.(Ref 14) obtained the velocity of the liquid metal in the sprue with the help of sensors placed in different mold designs (Al and SG 42 alloy) and compared them with simulation. Majidi and Beckermann (Ref 15) noted that during the filling of the casting mold, the air entrainment is effective in the formation of oxide and the vortex flow provides less oxide film formation in the mold. Kao et al.(Ref 16) investigated the effects of an asymmetric pouring basin to reduce the porosity in Al-Si7Mg(Fe) alloys and succeeded in reducing the porosity formation by 85%. Pavlak and Sturm (Ref 17) tried to minimize the oxide formations in aluminum casting with the autonomous design of experiments (DOEs) with Magmasoft program.

El-Sayed et al.(Ref 18) demonstrated that bifilms and porosity formed in Al and Mg alloys are interrelated. In many studies, the effect of the oxide film content of the cast material on the mechanical properties has been evaluated, especially by the Weibull analysis (Ref 7,12,18,19) and the quality index (Ref 20,21). The flow rate changes continuously at the beginning and end of the casting. Conservation of energy and the law of continuity is used in calculating the cross-sectional areas and flow rates of runner systems. Oxide film layers formed and developed due to the turbulence of the liquid metal, negatively affect the mechanical properties of the cast material. In addition, it reduces the effectiveness of other processes (grain refinement and modification) used to increase mechanical properties. It also conducts many studies on the oxide film thickness depending on the chemical composition (Ref 22–24).

Since there is no study on the effect of oxide films on mechanical properties due to casting geometry, this study was required. In the study, Al-Si-Mg alloy was poured into the square, rectangular, circle, and triangular (equilateral) mold cavities with equal volume and runner system. Quality indexes of Al-Si-Mg alloys produced in different mold cavities were evaluated by OM and SEM microstructure studies, tensile and hardness tests.

2. Materials and Method

The study used a core box to produce molds with the same runner system and different geometries. The molds were manufactured using silica sand, resin, and hardener. The mold cavity filling was recorded at 400 fps during casting using a CASIO FX-25 model camera to determine liquid metal movement and flow rate.

Components of the runner system used in the study and dimensions of cast parts with different geometries are shown in Fig. 1.a and the positions of tensile test and metallography specimens obtained from the intersection of cast parts with different geometries are given in Fig. 1. b. Metallography samples were prepared according to ASTM E3-11 standard, and then OM images were taken from 3 different samples from 5 different regions under an IMEJI brand optical microscope. The acquired OM images were processed in the MSQ plus program, and Secondary Dendrite Arm Spacing (SDAS) was calculated. The linear line intercept method was used to measure

the SDAS. Metallography samples in cast parts were taken from the regions closest to the center of gravity of the cast part. Two casting processes were carried out for tensile tests, and one casting was performed to determine liquid metal movement and flow rate. Tensile test samples were obtained parallel and perpendicular to the liquid metal flow direction. All casting material thicknesses were kept constant at 15 mm, and total mold cavity volumes at 375 cm^3. In the sprue, the effective casting height (over basin) is 0.035 m, the velocity of liquid metal is 0.83m / sec, and the upper area of the sprue is 4.35 cm^2. Depending on the velocity of the liquid metal and cross-sectional areas of the runner systems, the calculated flow rate of the liquid metal was calculated to be approximately 0.000361 m3/sec. These calculations ignored changes in the friction and the cross-sectional area between the liquid metal and the mold sand caused by pressure differences in the states of changing its shape.

Fig. 1.

Al-Si-Mg alloy used in the study was obtained from ingot. The result of its chemical composition obtained from the S3 MiniLAB 300 metal analysis spectrometer device found in Manufacturing Engineering Laboratories Karabuk University is given in Table 1. No degassing process was applied to Al-Si-Mg alloys. The pouring temperature of all the cast parts was between 730-740°C.

Table 1.

T6 heat treatment was applied to all casting materials to increase mechanical strength by precipitation hardening in Al-Si-Mg alloys. Microstructural examinations of the cast Al-Si-Mg alloys produced were carried out with Nikon brand optical microscope (OM) and Carl Zeiss Ultra Plus Gemini (FEG) (with EDS) scanning electron microscope (SEM). Macrohardness measurements were used in the AFFRI brand hardness device (by Brinell hardness criteria) with a loading time of 30 seconds under 2.5 mm ball diameter and 31.25 kg force. Macrohardness values were determined by averaging ten hardness measurements from each group. Tensile test samples for tensile tests were made by ASTM: B557M-10 standards in SHIMADZU AG-IS model tensile device with AG-IS 50 kN capacity at a speed of 1mm/min. The quality indexes of the casting geometry were calculated based on the average maximum tensile strength and percent elongation obtained. Quality index studies are given and used in Equation 1 for cast aluminum and its alloys in many studies (Ref 19,20,25–28).

$$Q_{index}(Q_i) = UTS(MPa) + 150\log(\varepsilon\%) \quad \text{.....(1)}$$

where the quality index is Q_{index}, the maximum tensile strength is UTS, and the elongation value is E%.

3. Results and Discussion

In this study, the effect of part geometries (square, rectangular, circle, and equilateral triangular) with equal cross-sectional area and volume casting on microstructural properties and mechanical properties were investigated on two bases. The first is the flow rate of liquid metal, and the second is the effect of casting defects on mechanical properties that develop due to the flow of liquid metal.

3.1. Effect of Flow Rate on Oxide Films

In the study, video images were obtained in real-time periods where the liquid metal filled the mold cavity of different geometries and then processed into photo frames at 0.25-second intervals. The image analysis program scanned instant photo frames, and time-dependent liquid metal volumes were calculated. The flow parameters and SDAS data obtained in mold cavities with different geometries are given in Table 2. According to the SDAS data,

the cooling rates of the cast parts and the local solidification times were similar. Considering the calculated flow rate and the volume of the mold cavity, it is necessary to fill the mold cavity in a short time, almost 1 second. However, this filling time could not be captured in any mold cavity geometry designed for liquid metal. Flow rates occurring in the mold cavity are quite low and different compared to the calculated flow rate. The actual flow rates are lower than the calculated flow rate because of the pressure created by the metal rising in the mold cavity, the friction with the sand, and the decrease in temperature. It has been observed that the flow rate of the liquid metal decreases due to these reasons. In addition, changing the direction of the liquid metal and changing the cross-sectional area are other parameters that affect the reduction of the flow rate. Therefore, the study aimed to determine the effect of liquid metal rising in the mold cavity from the flow rate at total casting time and time-dependent flow maps. Flow rate is an essential parameter for the casting production method. At the low velocity of liquid metal, the flow rate is low. Especially in metal die-casting, if the flow rate is low, the flowability of the liquid metal decreases, its oxidation and inclusion formation increase. This situation causes the flow of liquid metal to end. A high flow rate causes the metal mold to wear very quickly, and the surface quality of the casting part decreases. Paul et al. (Ref 29) simulated the instantaneous motion of the liquid metal in the mold cavity using two different methods, using Magmasoft and SPH (smoothed particle hydrodynamics). Experimentally, they tried to simulate the instantaneous liquid metal flow with water modeling. As a result, they emphasize that SPH modeling corresponds better with experimental water modeling. In other studies, the turbulence of the liquid metal and the surface turbulence (Ref 30), oxide film formation, and folding (Ref 31) were simulated with the SPH method. In addition, numerical methods and special software used in a study on the junction angle (40-90 ° deg.) between the horizontal runner and ingate cross-section determined that the casting time decreases with the increasing angle (Ref 32). The surface turbulence of the liquid metal is important not only in sand or metal casting but also in many special casting methods such as ceramic mold casting and tilt casting (Ref 33). The filtration of the liquid metal reduces the speed of the liquid metal and positively affects the mechanical strength (Ref 12,13); at the same time, even after the ceramic filter, the oxidation of the liquid metal continues and affects the mechanical strength depending on the height it falls (Ref 20).

Table 2.

Due to different mold cavity geometries, the irregularity (increase or decrease) in liquid metal flows occurs. This leads the turbulence and surface turbulence in the liquid metal. The OM images taken from Al-Si-Mg samples with different mold geometry are shown in Fig. 2. α-Al dendrites (Fig. 2a), Si eutectic (Fig. 2b), and Al5FeSi intermetallic developed during solidification were seen in the OM images. In addition, porosities between α-Al dendrites were seen (Fig. 2 a, c and d). Many studies have stated that the microstructure is affected similarly depending on the solidification rate and alloying element during the solidification of Al-Si-Mg alloys (Ref 34,35).

Fig. 2.

Fig. 3.a shows time-dependent volume changes of cast parts with different geometries. In this Fig. 3.a, the sudden increase or decrease in the volume of the liquid metal over time shows that the liquid metal is oxidized. Fig. 3.b represents fitted lines for different mold cavities. In the triangular mold cavity, the cross-sectional area decreases depending on the height, while the square cross-sectional area is constant. For this reason, flow photos were selected in the time periods when the flow rate changed. Selected liquid metal images depending on the time of casting parts with different geometry are shown in Fig. 4.

Fig. 3.

The flow images obtained in the time periods in which the flow rate suddenly changes in Fig. 3 are given in Fig. 4. Liquid metal flows depending on the casting mold geometry and time are given (Fig. 4). It was determined that the protective oxide film layer on the surface of the liquid metal filling the mold cavity was folded over each other, and new oxide films were formed.

Surface turbulence negatively affects the mechanical properties at least as much as bulk turbulence. It is seen that a small amount of liquid reaches the square and circular mold cavities in time periods of 0.75-1.25 sec. On the other hand, it is seen that a higher volume of liquid reaches the liquid metal in rectangular and equilateral triangular mold cavities. However, it is seen that the liquid metal enthusiastically transforms into the square-mold cavity in 1.00-1.75 sec. Then, it is seen that the square mold cavity is filling up quite calmly for about 3.25 sec. It was determined that the oxide film layer on its surface was continuously broken, and new oxide films were formed in the circular mold cavity in the range of 1.00-3.25 seconds. It was determined that the filling ratio of the rectangular mold cavity in 1.25- 4.00 sec. was quite low, and the folding on the liquid surface is repeated along its long side. Reilly et al. indicate that the liquid metal folds on itself continuously when it takes for the horizontal runner system to be completely filled with liquid metal (transition time) (Ref 36). Kheirabi et al. stated that in the unpressurized runner system when the ingate is at the bottom, vortex flow regions in the liquid metal and turbulence on the surface of the liquid metal (Ref 37). It is seen that the filling ratio of the equilateral triangular mold cavity is higher than the rectangular and circular mold cavities. This is explained by narrowing the cross-sectional area in which the liquid metal is filled, thus increasing the amount of rising of the liquid metal. The same situation is clearly seen in the circular mold cavity in 1.00-1.75 sec. time interval. Starting from the preparation of the liquid metal, the charge metal, the melting furnace, and equipment used, the crucible used to transport the liquid metal and the atmospheric conditions that cause the oxidation of the liquid metal (Ref 1–3,17). In addition to these, the liquid metal constantly changes speed, friction, and turbulence (bulk and surface) in the runner system. It has been stated in many studies that liquid metal with turbulence and surface turbulence reduces the mechanical strength of the cast material (Ref 6,9,11). There are many studies examining the effects of turbulence and surface turbulence in the runner system of liquid metal on the mechanical. It is emphasized that the folding of the protective oxide film, the formation of a new oxide layer, and its repetition during the filling process negatively affect the mechanical properties regardless of the casting method (gravity, permanent, etc.)(Ref 5,7,11,31,38–41).

Fig. 4.

3.2. Effect of Flow Rate on Mechanical Properties

The effect of the geometry of the mold cavity on mechanical properties was investigated by the arithmetic mean of the ultimate tensile strength and percent elongation data. Fig. 5 shows the ultimate tensile strength and percent elongation depending on the geometry of the mold cavity.

According to the tensile test results obtained, the average ultimate tensile strength and elongation are as follows, respectively $\sigma_{square} > \sigma_{equilateral\ triangle} > \sigma_{rectangle} > \sigma_{circle}$ and $\varepsilon_{square} > \varepsilon_{equilateral\ triangle} > \varepsilon_{rectangle} > \varepsilon_{circle}$. The highest maximum ultimate tensile strength and percent elongation occurred in the cast material with square geometry. In contrast, the cast material with circular geometry had the lowest ultimate tensile strength and percent elongation. However,

it is clear that the frequency of tensile strengths of cast Al-Si-Mg alloy is very different, depending on the mold cavity geometry.

Fig. 5.

The quality indexes, average macrohardness results, range, and standard deviations of cast materials with different mold cavity geometry are given in Table 3. The hardness values obtained are not affected by the geometry of the mold cavity. The cast Al-Si-Mg alloys' tensile test results and quality indexes produced in different mold cavity geometries change significantly depending on the liquid metal flow rate. The square geometry mold cavity reveals the highest properties, as seen in Fig. 5. The scatter of the results is also very low. The interesting point in the mechanical properties is that the error bars are scattered broadly, yet all the geometry has the potential to 330 quality indices. This highest value was somehow reached in each geometry. This shows the potential property of the alloy. However, if the mold cavity is not filled quiescently, then the mechanical properties drop significantly. It is not the microstructure or the heat treatment, but the casting quality is the crucial parameter. The horizontal cross-section area of the four different geometries changes as the liquid metal moves in the mold cavity. Since the entry cross-section area is the smallest for the circle mold cavity geometry, the highest turbulence is observed (as can be seen in Fig. 4). Therefore, it reveals the lowest quality index. For triangular mold cavity geometry, the entrance cross-section area is high, leading to slower filling; however, as the geometry gets smaller when the liquid moves upwards, the velocity increases. As shown in Fig. 6, the velocity of the liquid in triangular mold cavity geometry goes above the critical velocity and reaches 1 m/s. This continued increase in velocity results in the entrainment of surface oxide towards the top of the casting. Therefore, the mechanical properties are highly scattered in this geometry.

On the other hand, in rectangular mold cavity geometries, since the cross-area does not change in the mold cavity, more quiescent filling and high tensile properties with the lowest scatter are observed. Tiryakioglu et al. compared the methods for calculating the quality index for aluminum alloys and discussed their deficiencies (Ref 42). Another study noted that the yield strength and elongation values of Al-7 pct Si-Mg alloy obtained from the literature were linearly fit for maximum data. Still, the scattering of the test results was due to defects caused by the casting method (Ref 21). Therefore, in Al-Si-Mg alloy poured into different mold cavities, it was observed that while the maximum UTS, e%, and Qi data are almost close to each other, the minimum values change significantly.

Fig. 6.

Table 3.

Fig. 7.

In Fig. 7, survivability plots are given. The statistical analysis shows a similar trend for UTS, elongation at fracture, and quality index values. The square mold cavity reveals the highest reproducible and reliable mechanical properties, whereas the circle is the worst. As seen in Fig. 7a triangle, circle, and rectangle mold cavities have the potential to give UTS values below 50 MPa. On the other hand, square geometry reveals a minimum of 100 MPa. In Fig. 7b, when the square mold cavity is used, it does not break under 6% elongation. Thus, this geometry will have a minimum of 6% elongation at fracture below which no fracture will be observed. The same applies to elongation at fracture and quality index values (Fig. 7c). Based on the survivability plots in Fig. 6, this alloy can show up to 14% elongation under these conditions, almost half of what Tiryakioglu (Ref 42) claims this alloy can reveal as the highest fracture of 29%.

In Fig. 8, SEM images taken from cast materials with rectangular mold cavities (Fig. 8a) and square mold cavities (Fig. 8b), and chemical compositions obtained from EDS analysis are given. In the structure, aluminum with dendritic morphology, Si eutectic in lamellar morphology, and Al-Si-Fe intermetallic in plate or lath morphology were determined.

Fig. 8.

In Fig. 9, SEM images and EDS analysis of the fracture surfaces after the tensile test are given. It has been determined that the sizes of aluminum dendrites are almost close to each other, depending on the different casting geometry on fracture surfaces.

However, it is seen that there are bifilm oxides trapped between dendrites on fracture surfaces, and they cause fracture (in Fig. 9a. 1, Fig. 9b. 1, Fig. 9c. 3). Al-Si-Fe intermetallic compound was determined at the points in Fig. 9a. 1, Fig. 9b. 1, Fig. 9c. 1. Especially in Fig. 9d. 1, it is seen that the bifilm is quite wrinkled and incompatible.

The primary phases in the microstructure of A356/357 alloys consist of dendritic aluminum matrix, Al-Si eutectic, and AlSiFe intermetallic. At the same time, A356/357 alloys can be strengthened with Mg content and Mg_2Si precipitates by T6 heat treatment. The modification process's cooling rate and the morphology of the phases forming the microstructure directly affect the mechanical properties (Ref 43). Tensile test results improve with the increase of precipitate intermetallic phases formed with the amount of Mg (Ref 44). Depending on the amount of Fe, the fraction of Al5FeSi and Al8Fe2Si intermetallic in the structure changes, and the tensile test results deteriorate with the increase of the Al5FeSi intermetallic fraction (Ref 45).

Fig. 9.

4. Conclusion

This study produced Al-Si-Mg alloy in different geometries (square, rectangular, circle, and equilateral triangular) with equal mold cavity volume. The effect of part geometry on the microstructural and mechanical properties of the alloy was investigated, and the following results were obtained.

- Depending on the mold cavity geometry, the velocity of the liquid metal and the turbulence tendency change with the change in the cross-section area of the mold cavity.
- Flow rate and total casting time were different in mold cavities with equal volume and different geometries, mainly due to the difference in the cross-section. Measurements of SDAS of Al-Si-Mg alloys poured into casting cavities with different geometries are almost close to each other.
- While the highest mechanical strength and quality index was obtained in the square mold cavity, the lowest mechanical strength and quality index was obtained in the circular mold cavity. It has been

determined that the change in the velocity and turbulence of the liquid metal depending on the mold cavity geometry is the reason for this situation.

- The tensile strength and quality index increase with the increase in flow rate stability.
- It has been determined that bifilms are wrinkled and incoherently squeezed between dendrites and Al-Si-Fe intermetallic nucleated, especially around bifilms.

Acknowledgments

The authors gratefully wish to acknowledge the financial support of the Karabuk University Science Research Department (KBUBAP-18-YL-148).

References

1. J. Campbell, "Complete Casting Metal Casting Processes, Metallurgy, Techniques and Design," First edit, (Oxford), Butterworth-Heinemann, 2011.
2. J. Campbell, "Castings Practice: The Ten Rules of Castings," *Butterworth-Heinemann*, First edit, (Oxford), Elsevier Ltd, 2004.
3. D. Dispinar and J. Campbell, Porosity, Hydrogen and Bifilm Content in Al Alloy Castings, *Mater. Sci. Eng. A*, Elsevier B.V., 2011, **528**(10–11), p 3860–3865, doi:10.1016/j.msea.2011.01.084.
4. M. Divandari and J. Campbell, Oxide Film Characteristics of Al-7Si-Mg Alloy in Dynamic Conditions in Casting, *Int. J. Cast Met. Res.*, 2004, **17**(3), p 182–187.
5. M. Divandari and J. Campbell, Morphology of Oxide Films of Al-5Mg Alloy in Dynamic Conditions in Casting, *Int. J. Cast Met. Res.*, 2005, **18**(3), p 187–192.
6. X. Yang, T. Din, and J. Campbell, Liquid Metal Flow in Moulds with Off-Set Sprue, *Int. J. Cast Met. Res.*, 1998, **11**(1), p 1–12.
7. N. Green and J. Campbell, Influence of Oxide Film Filling Defects on the Strength of Al-7Si-Mg Alloy Castings., *AFS Trans.*, 1994, **102**(January), p 341–347.
8. F.Y. Hsu, M.R. Jolly, and J. Campbell, Vortex-Gate Design for Gravity Casting, *Int. J. Cast Met. Res.*, 2006, **19**(1), p 38–44.
9. F.Y. Hsu and H.J. Lin, A Diffusing Runner for Gravity Casting, *Metall. Mater. Trans. B Process Metall. Mater. Process. Sci.*, 2009, **40**(6), p 833–842.
10. F.Y. Hsu, M.R. Jolly, and J. Campbell, A Multiple-Gate Runner System for Gravity Casting, *J. Mater. Process. Technol.*, 2009, **209**(17), p 5736–5750.
11. T. Tunçay, S. Tekeli, and D. Özyürek, Effect of Diffuser and Non-Diffuser Runner Systems on the Mechanical Properties of A356 Alloy, *J. Fac. Eng. Archit. Gazi Univ.*, 2013, **28**(2), p 241–249.
12. T. Tunçay and D. Özyürek, The Effects on Microstructure and Mechanical Properties of Filtration in Al-Si-Mg Alloys, *J. Fac. Eng. Archit. Gazi Univ.*, 2014, **29**(2), p 271–279.
13. F.Y. Hsu and C.L. Li, Runner Systems Containing Ceramic Foam Filters Quantified by "Area Normalized" Bifilm Index Map, *Int. J. Met.*, 2015, **9**(3), p 23–35.

14. K. Metzloff, K. Mageza, and D. Sekotlong, Velocity Measurement and Verification with Modeling of Naturally Pressurized Gating Systems, *Int. J. Met.*, Springer International Publishing, 2020, **14**(3), p 610–621, doi:10.1007/s40962-020-00471-w.

15. S.H. Majidi and C. Beckermann, Effect of Pouring Conditions and Gating System Design on Air Entrainment During Mold Filling, *Int. J. Met.*, Springer International Publishing, 2019, **13**(2), p 255–272, doi:10.1007/s40962-018-0272-x.

16. Y.C. Kao, H.W. Tseng, M.H. Ho, K.Y. Liang, Y.G. Liu, Y. Bin Yang, C.H. Lee, and Y.K. Fuh, Prediction of the Effect of Asymmetric Pouring Basin Geometry on Temperature, Internal Porosity in Tilt Casting Housing of Scroll Compressor, *Int. J. Met.*, Springer International Publishing, 2021, doi:10.1007/s40962-021-00659-8.

17. L. Pavlak and J.C. Sturm, Reduction of Oxide Inclusions in Aluminum Cylinder Heads through Autonomous Designs of Experiments, *Int. J. Met.*, Springer International Publishing, 2017, **11**(2), p 174–188.

18. M.A. El-Sayed, H. Hassanin, and K. Essa, Bifilm Defects and Porosity in Al Cast Alloys, *Int. J. Adv. Manuf. Technol.*, The International Journal of Advanced Manufacturing Technology, 2016, **86**(5–8), p 1173–1179, doi:10.1007/s00170-015-8240-6.

19. H.R. Ammar, A.M. Samuel, F.H. Samuel, and H.W. Doty, The Concept of Quality Index and Its Application for Al–Si Cast Alloys, *Int. J. Met.*, Springer International Publishing, 2021, (November 2020), doi:10.1007/s40962-020-00556-6.

20. G. Eisaabadi Bozchaloei, N. Varahram, P. Davami, and S.K. Kim, Effect of Oxide Bifilms on the Mechanical Properties of Cast Al-7Si-0.3Mg Alloy and the Roll of Runner Height after Filter on Their Formation, *Mater. Sci. Eng. A*, Elsevier B.V., 2012, **548**, p 99–105, doi:10.1016/j.msea.2012.03.097.

21. M. Tiryakioğlu, J. Campbell, and N.D. Alexopoulos, On the Ductility of Cast Al-7 Pct Si-Mg Alloys, *Metall. Mater. Trans. A Phys. Metall. Mater. Sci.*, 2009, **40**(4), p 1000–1007.

22. M.M. Jalilvand, N.T. Bagh, M. Akbarifar, and M. Divandari, A New Insight to Dynamic Oxidation of Molten Metals by the Parametric Study of Oxide/Metal/Oxide Sandwich Formation, *Int. J. Met.*, Springer International Publishing, 2020, **14**(4), p 949–961, doi:10.1007/s40962-019-00395-0.

23. N. Taheri Bagh, M. Divandari, M. Shahmiri, and M. Akbarifar, Characteristics of Dynamically Formed Oxide Films in Al–Zn Melt, *Int. J. Met.*, Springer International Publishing, 2021, **15**(3), p 747–762, doi:10.1007/s40962-020-00501-7.

24. B. Nayebi and M. Divandari, Characteristics of Dynamically Formed Oxide Films on Molten Aluminium, *Int. J. Cast Met. Res.*, 2012, **25**(5), p 270–276.

25. M. Tiryakioğlu and J. Campbell, Weibull Analysis of Mechanical Data for Castings: A Guide to the Interpretation of Probability Plots, *Metall. Mater. Trans. A Phys. Metall. Mater. Sci.*, 2010, **41**(12), p 3121–3129.

26. M. Uludağ, R. Çetin, D. Dişpinar, and M. Tiryakioğlu, On the Interpretation of Melt Quality Assessment

of A356 Aluminum Alloy by the Reduced Pressure Test: The Bifilm Index and Its Physical Meaning, *Int. J. Met.*, 2018, **12**(4), p 853–860.

27. L. Alyaldin, M.H. Abdelaziz, A.M. Samuel, H.W. Doty, S. Valtierra, and F.H. Samuel, Effects of Alloying Elements and Testing Temperature on the Q-Index of Al–Si Based Alloys, *Int. J. Met.*, Springer International Publishing, 2018, **12**(4), p 839–852, doi:10.1007/s40962-018-0215-6.

28. G. Sigworth, Understanding Quality in Aluminum Castings, *Int. J. Met.*, 2011, **5**(1), p 7–22.

29. P. Cleary, J. Ha, V. Alguine, and T. Nguyen, Flow Modelling in Casting Processes, *Appl. Math. Model.*, 2002, **26**(2), p 171–190.

30. J.P. Morris, Simulating Surface Tension with Smoothed Particle Hydrodynamics, *Int. J. Numer. Methods Fluids*, 2000, **33**(3), p 333–353.

31. X. Yang, X. Huang, X. Dai, J. Campbell, and J. Tatler, Numerical Modelling of Entrainment of Oxide Film Defects in Filling of Aluminium Alloy Castings, *Int. J. Cast Met. Res.*, 2004, **17**(6), p 321–331.

32. S. Sulaiman and T.C. Keen, Flow Analysis along the Runner and Gating System of a Casting Process, *J. Mater. Process. Technol.*, 1997, **63**(1–3), p 690–695.

33. L.F. Pease, J. Bao, R. Safarkoolan, T.G. Veldman, N.R.J. Phillips, P.S. McNeff, and C.K. Clayton, Flow Obstacles Minimize Surface Turbulence in Tilt Casting, *Chem. Eng. Sci.*, Elsevier LTD, 2020, **230**, p 116104, doi:10.1016/j.ces.2020.116104.

34. S. Thompson, S.L. Cockcroft, and M.A. Wells, Advanced Light Metals Casting Development: Solidification of Aluminium Alloy A356, *Mater. Sci. Technol.*, 2004, **20**(2), p 194–200.

35. T.H. Ludwig, P.L. Schaffer, and L. Arnberg, Influence of Some Trace Elements on Solidification Path and Microstructure of Al-Si Foundry Alloys, *Metall. Mater. Trans. A Phys. Metall. Mater. Sci.*, 2013, **44**(8), p 3783–3796.

36. C. Reilly, N.R. Green, and M.R. Jolly, Surface Oxide Film Entrainment Mechanisms in Shape Casting Running Systems, *Metall. Mater. Trans. B Process Metall. Mater. Process. Sci.*, 2009, **40**(6), p 850–858.

37. A. Kheirabi, A. Baghani, A. Bahmani, M. Tamizifar, P. Davami, M. Ostad Shabani, and A. Mazahery, Understanding the Occurrence of the Surface Turbulence in a Nonpressurized Bottom Gating System: Numerical Simulation of the Melt Flow Pattern, *Proc. Inst. Mech. Eng. Part L J. Mater. Des. Appl.*, 2018, **232**(3), p 230–241.

38. F. Bahreinian, S.M.A. Boutorabi, and J. Campbell, Critical Gate Velocity for Magnesium Casting Alloy (ZK51A), *Int. J. Cast Met. Res.*, 2006, **19**(1), p 45–51.

39. D.Z. Li, J. Campbell, and Y.Y. Li, Filling System for Investment Cast Ni-Base Turbine Blades, *J. Mater. Process. Technol.*, 2004, **148**(3), p 310–316.

40. R. Gopalan and N.K. Prabhu, Oxide Bifilms in Aluminium Alloy Castings - A Review, *Mater. Sci. Technol.*, 2011, **27**(12), p 1757–1769.

41. X. Dai, X. Yang, J. Campbell, and J. Wood, Effects of Runner System Design on the Mechanical

Strength of Al-7Si-Mg Alloy Castings, *Mater. Sci. Eng. A*, 2003, **354**(1–2), p 315–325.

42. M. Tiryakioğlu, J. Campbell, and N.D. Alexopoulos, Quality Indices for Aluminum Alloy Castings: A Critical Review, *Metall. Mater. Trans. B Process Metall. Mater. Process. Sci.*, 2009, **40**(6), p 802–811.

43. Q.G. Wang, Microstructural Effects on the Tensile and Fracture Behavior of Aluminum Casting Alloys A356/357, *Metall. Mater. Trans. A Phys. Metall. Mater. Sci.*, 2003, **34**(12), p 2887–2899.

44. M. Yildirim and D. Özyürek, The Effects of Mg Amount on the Microstructure and Mechanical Properties of Al-Si-Mg Alloys, *Mater. Des.*, 2013, **51**, p 767–774.

45. T. Tunçay and S. Bayoğlu, The Effect of Iron Content on Microstructure and Mechanical Properties of A356 Cast Alloy, *Metall. Mater. Trans. B Process Metall. Mater. Process. Sci.*, 2017, **48**(2), p 794–804.

Captions of Figure and Table

Figures

Fig. 1. The runner system used in the study and the dimensions of different mold cavity geometries (a); the dimensions of the tensile specimens (b), (All dimensions are in mm).

Fig. 2. The OM images of Al-Si-Mg alloys poured into (a) rectangular; (b) square; (c) triangular (equilateral); and (d) circular mold cavities.

Fig. 3. Volumetric change of liquid metal poured into different mold cavities, (a) time dependent volumetric levels; (b) fitted lines for different mold cavities.

Fig. 4. Filling conditions of liquid metal poured into different mold cavities at certain moments.

Fig. 5. The average ultimate tensile stress (a); strain (b); and quality indexes (c) depending on the mold cavities.

Fig. 6. Change in velocity of the liquid front as it rises in the mold cavity.

Fig. 7. Survivability plots of (a) UTS; (b) elongation at fracture; (c) Quality index

Fig. 8. SEM images of alloys poured into rectangular (a); and square (b) mold cavities.

Fig. 9. SEM images of fracture surfaces of alloys poured into (a) rectangular; (b) square; (c) triangular (equilateral); and (d) circular mold cavities.

Tables